Putative tumor metastasis-associated genes in human gastric cancer

TSUNG-FAN TUAN[1,2], CHENG-TA CHUNG[2,3], HSIAO-HUI TSOU[4], FONG-WEN CHEN[2,5], HENG-LIANG LIN[2], YIU-KAY LAI[3], WEN-SEN LEE[1], YU-SHENG CHAO[2], LING-LING HWANG[1] and CHIUNG-TONG CHEN[1,2,5]

[1]Graduate Institute of Medical Sciences, College of Medicine, Taipei Medical University, Taipei; [2]Institute of Biotechnology and Pharmaceutical Research, National Health Research Institutes, Miaoli; [3]Institute of Biotechnology, National Tsing Hua University, Hsinchu; [4]Division of Biostatistics and Bioinformatics, Institute of Population Health Sciences, National Health Research Institutes, Miaoli; [5]Graduate Institute of Life Sciences, National Defense Medical Center, Taipei, Taiwan, R.O.C.

Received March 4, 2012; Accepted May 11, 2012

DOI: 10.3892/ijo.2012.1502

Abstract. Gastric cancer is one of the leading causes of cancer mortality and its malignancy, resulting from disseminated cancer cells of diffuse type, is clinically manifested as metastases to the liver and peritoneum. The aim of the present study was to identify putative tumor metastasis-associated genes in human gastric cancer cells of diffuse type. An MKN45 cell line constitutively expressing green fluorescent protein (MKN45-GFP) was established and selected using the Transwell® system for invasive sublines MKN45-GFP-4, MKN45-GFP-10 and MKN45-GFP-12. MKN45-GFP-10 and MKN45-GFP-12 are highly invasive compared to the others. The mRNA levels were measured with cDNA microarrays and correlated with their invasion abilities in these sublines. Many of the genes identified with a positive or negative correlation are associated with angiogenesis, cell cycle, cytoskeleton and cell motility, protease and cell adhesion, as well as cellular signal transduction. In particular, novel genes without known functions were also noted. RT-PCR and western blot analyses were applied to verify the expression of selective genes. Following orthotopical intraperitoneal implantation, MKN45-GFP-12 demonstrated significantly higher *in vivo* tumor malignancies than parental MKN45-GFP in ascites induction and liver -invasion in mice. We have identified putative gastric tumor metastasis-associated, as well as novel genes. These genes and their protein products are to be further explored for their functional roles associated with tumor metastasis. The molecular profiles of these identified genes, gene transcripts and proteins in the patient specimens are likely to be useful biomarkers for diagnostic, therapeutic and/or prognostics. Most importantly, they may be used as molecular targets for the discovery of antitumor drugs against human gastric cancer metastasis.

Correspondence to: Dr Chiung-Tong Chen, Institute of Biotechnology and Pharmaceutical Research, National Health Research Institutes, 35 Keyan Road, Zhunan, Miaoli 35053, Taiwan, R.O.C.
E-mail: ctchen@nhri.org.tw

Dr Ling-Ling Hwang, Graduate Institute of Medical Sciences, School of Medicine, Taipei Medical University, 250 Wu-Hsing Street Sinyi, Taipei 11031, Taiwan, R.O.C.
E-mail: llhwang@tmu.edu.tw

Key words: gastric cancer, invasion, metastasis, microarray, orthotopic implantation

Introduction

Gastric cancer is one of the most common types of human cancer (1) and the second most common cause of cancer mortality in the world (2). Gastric cancer has a wide variation in geographical distribution and the incidence is particularly high in Asia, South America and Eastern Europe (3-5). Gastric cancer patients are frequently diagnosed in advanced stages. Approximately 50% of all patients present with unresectable, locally advanced or metastatic diseases (6,7) and recurrence after curative gastrectomy remains high (8,9). The prognosis for patients with advanced gastric cancer remains dismal, and little improvement in the survival rates has been achieved in recent years (6,8,9). Gastric tumor metastases, during which the cancer cells spread to distal sites such as the liver, omentum, and lymph nodes, are the leading cause of cancer mortality. Gastric tumor of diffuse type is poorly differentiated and comprises dissemination-prone gastric cancer cells lacking the abilities of tissue cohesion and gastric biological functions. This particular type of gastric cancer cells demonstrates an increased propensity for metastatic spread via the intra- and trans-peritoneal wall and, therefore, have been associated with poor prognosis (7). The somatic inactivation of E-cadherin in diffuse type gastric cancer also increases epithelial-mesenchymal transition (EMT) ability and leads to an enhanced metastasis potential of this gastric cancer type (10). There is currently no effective chemotherapeutics, nor is a molecular-targeted drug available, for treating the advanced

gastric cancerous diseases. Further research into molecular targeting drugs against gastric tumor metastasis is warranted.

In the search for target molecules for the development of anticancer drugs, research efforts to identify biological molecules involved in the gastric cancer cell specific proliferation, invasion and metastasis have been extensive. Elevated plasma osteopontin was associated with gastric cancer development and patient survival (11). Overexpression of c-met (12), LOXL2 (13), EGFR (14), HER2 (15), TNS4 (16) and phosphorylated mTOR (17) in gastric tumors has been well correlated with the prognostic factors of tumor staging, the depth of tumor invasion and/or lymph node metastasis. On the other hand, reduced expressions of nm23 (18), galectin-3 (19), or TIP30 (20), loss of RUNX3 (21) or E-cadherin (14) expressions, and abnormal expression of E-cadherin (22) in gastric tumors has been associated with gastric tumor metastasis and poor prognosis. More systemically investigated, array-based technologies were utilized to analyze and identify genes associated with gastric cancer metastasis. Several studies compared human primary to metastatic gastric cancer cell lines (23,24), human gastric cancer cell lines to a normal gastric cell line (25), unpaired tumors to normal tissues (26), paired patient gastric tumors to normal gastric tissues (25,27-31), and patient gastric tumors with different clinical stages (32). However, differences in the genomic backgrounds of patients and the mix of the tumor and its surrounding cells may increase the complexities and difficulties for the identification of specific genes and for database analyses. Results of these array-based studies individually suggested that putative metastasis-associated genes are not entirely the same, nor are they similar, to a great extent, to each other. Further studies are, therefore, needed to identify biologically relevant molecular targets against which effective drugs for human gastric cancer may be discovered.

In the present study, we generated, from a single parental cell, a set of cell sublines exhibiting different metastatic abilities and used them to identify the genes whose expression levels are correlated to their metastatic abilities. We applied a genome-wide scale cDNA microarray analysis using a biological functional approach different from those previously reported. A human gastric cancer cell MKN45 originally derived from a poorly differentiated gastric adenocarcinoma of the stomach of a 62-year-old woman (33,34) was used as a model cell for its diffuse phenotype potentially prone to metastasis. A series of the human gastric cancer MKN45 cell subclones with varying invasion capabilities were established. A number of putative tumor metastasis-associated genes were identified using cDNA microarray analysis and verified with correlated mRNA levels and protein expressions.

Materials and methods

Cell line and transfection. The human diffuse-type gastric cancer cell line MKN45 (JCRB0254) was purchased from the Japanese Collection of Research Bioresources/Human Science Research Resources Bank (Osaka, Japan). The cells were grown in RPMI-1640 medium (Gibco, product no. 31800105) with 10% fetal bovine serum (FBS) (Invitrogen, Carlsbad, CA, USA) and 2 mM L-glutamine at 37˚C, 5% CO_2. One day before the transfection, $8x10^3$ MKN45 cells were seeded into 24-well culture plate and grown for 16-24 h to 70-90% confluence for transfection. A mixture of enhanced green fluorescent protein (GFP) expression plasmid (pEGFP-C1, cat. no. 6084-1) encoding under the control of cytomegalovirus promoter, OPTI-MEM and Lipofectamine™ 2000 from Invitrogen at a ratio of 2 μg:2 μl:100 μl was added to the MKN45 cells. The cells were harvested following incubation for 48 h at 37˚C followed by selection of the GFP-expressing clones by incubating with 1 mg/ml G418 (Invitrogen) and isolated with limiting dilution method to obtain stably GFP-expressing MKN45-GFP sublines.

Selection of highly invasive MKN45-GFP sublines. The MKN45-GFP cells of the isolated clone were selected for differential invasive characteristics using Transwell® plates from Corning (Acton, MA, USA) with a method modified from one previously described (35) Briefly, Transwell of the 24-well inserts with semi-permeable polycarbonate membrane (8 μm in pore size, Corning, cat. no. CLS3422, Corning, NY, USA) were coated with 50 μl per well of reconstituted basement-membrane matrix Matrigel™ (1:1 diluted with growth medium) from BD Biosciences (San Jose, CA, USA). MKN45-GFP cells in RPMI-1640 containing 10% FBS were seeded at $1x10^5$ cells/200 μl/well onto the upper surface of the Matrigel-coated membrane. Following incubation for 72 h at 37˚C, the inserts were removed. The cells that migrated and invaded through the membrane and attached to the surface of bottom well were harvested aseptically and subsequently amplified for further selection processes. The harvested invasive MKN45-GFP cell sublines after each selection round were named with a number correspondingly.

In vitro invasion assay. The basement membrane matrix coated Transwell system was used to measure the invasion ability of tumor cells as previously reported (36). Transwell of 24-well plates with a porous polycarbonate membrane of 8-μm pore size from Corning (Corning, NY) were coated with 50 μl Matrigel diluted (1:20 = v:v) with RPMI-1640 culture medium. Cells ($5x10^5$) suspended in 200 μl RPMI-1640 with 1% FBS were seeded into upper chamber. The lower chamber was placed with 600 μl RPMI-1640 with 10% FBS. Following incubation for 72 h at 37˚C, the cells that invaded through the Matrigel-coated membrane to the lower surface of the membrane and the bottom surface of the culture well were fixed with 3.7% formaldehyde in phosphate-buffered saline (PBS) for 1 h. The cells that remained on the upper surface of the membrane were scraped with a cotton bud completely and invaded cells attached on the opposite surface of the membrane in the lower chamber were stained with hematoxylin for 1 h. The invaded cancer cells were then visualized and counted from 5 different viewing areas under 100-fold magnification using a DM IRB inverted microscope from Leica Microsystems (Wetzlar, Germany).

Cell proliferation activity. Cancer cell proliferation activity was measured using a colorimetric 3-(4,5-dimethylthiazol-2-yl)-5-(3-carboxymethoxyphenyl)-2-(4-sulfophenyl)-2H-tetrazolium salt (MTS)/phenazine methosulfate (PMS) assay system as previously reported (37). Cancer cells were seeded at 2,000, 4,000, and 6,000 cells/well in 96-well culture plates (Corning, Acton, MA) in triplicates. The cells were harvested

and the cell numbers were measured every 24 h or 6 consecutive days by a colorimetric reaction using MTS/PMS mixture, 2 mg/ml MTS (Promega, Madison, WI, USA) and 0.38 mg/ml PMS (Sigma, St. Louis, MO, USA), in phenol red-free RPMI-1640 medium (Gibco, product no. 11835-030) followed by optical density measurements at 490 nm after a 90-min incubation at 37˚C. The cell doubling time was obtained by nonlinear regression with the equation: $N=A_o*2\text{^}(T/T_d)$ using SigmaPlot® from SPSS Inc. (Chicago, IL, USA), in which N is the total cell number at time T; A_o is the initial cell number; and T_d is the cell doubling time.

Orthotopic tumor growth and metastasis in nude mice. Adult male athymic Nu-Fox1^{nu} nude mice purchased from BioLasco (Ilan, Taiwan) were housed in sterilized cages under 12-h light/dark cycles with water and food *ad libitum*. As previously described (38), nude mice were intraperitoneally inoculated with $5x10^6$ MKN45-GFP or MKN45-GFP-12 cells/mouse, suspended in 0.2 ml phenol-red free RPMI-1640 medium using 24G syringe needles at 35 nude mice per cancer cell type. After cancer cell inoculation, the occurrence of ascites was monitored weekly. The progression of the tumor growth was monitored by a fluorescence stereomicroscope MZ FLIII from Leica and animal body weights were recorded twice a week. GFP-expressing tumors were visualized with a D470/40x bandpass filter and a 495 DCLP dichroic filter. On the second week after the inoculation, 7 nude mice per cell type were euthanized weekly and the disseminated and metastasized tumors growing in the peritoneal cavities were visualized after laparotomy and the numbers of tumor nodules were counted using a fluorescent imaging system LT-9500 Illumatool TLS from Lightools Research (Encinitas, CA, USA). Metastasized tumors that had invaded into the livers of the nude mice were surgically removed and sectioned for microscopic examination following hematoxylin and eosin staining. The use of the animals was approved by The Institutional Animal Care and Use Committee of The National Health Research Institutes.

cDNA microarray assay. Total RNAs were isolated from the cancer cells using TRIzol® reagent (product no. 15596026, Invitrogen) according to the manufacturer's protocol. The purified RNA was quantified in optical density at 260 nm by an ND-1000 spectrophotometer from Nanodrop Technology (Wilmington, DE, USA) and qualified by Agilent 2100 Bioanalyzer. Total RNA of 0.5 μg was amplified by a low RNA input fluorescent linear amplification kit (cat. no. 5184-3523) from Agilent Technologies (Santa Clara, CA, USA) using Cyanine 3 (Cy3)-labeled CTP (cat. no. NEL580001EA) or Cyanine 5 (Cy5)-labeled CTP (cat. no. NEL581001EA) from Perkin Elmer (Waltham, MA, USA) during the *in vitro* transcription. The cancer cell RNAs were labeled with Cy5 and Universal Human Reference RNAs (cat. no. 636538) from Clontech (Mountain View, CA, USA) were labeled with Cy3. The Cyanine-labeled RNAs (cRNAs) of 2 μg were fragmented to an average size of 50-100 nucleotides by incubation with fragmentation buffer at 60˚C for 30 min. The fragmented labeled cRNAs were then pooled and hybridized to Human 1A Oligo Microarray (V2) from Agilent Technologies at 60˚C for 17 h. After they were washed, the arrays were dried using a nitrogen-filled air gun and scanned with Agilent dual DNA microarray scanner at 535 nm for Cy3 and 625 nm for Cy5, respectively. The scanned images were extracted by Feature Extraction 8.1 from Agilent Technologies and analyzed to quantify signal and background intensity and to substantially normalize the data by rank-consistency-filtering LOWESS method. The microarray data, including 4 analyzed samples (MKN45-GFP, MKN45-GFP-4, MKN45-GFP-10, and MKN45-GFP-12), have been deposited to the Gene Expression Omnibus (GEO; http://www.ncbi.nlm.nih.gov/geo/; accession number GSE33570).

RT-PCR analysis. Samples of the total RNA (1-5 μg) from the cancer cells were reverse-transcribed in a total volume of 20 μl by the SuperScript III First-Strand Synthesis System (cat. no. 18080-400) from Invitrogen. The reverse transcription products (1 μg) were used directly for PCR amplification. PCR amplification was performed with the PCR Reagent System (cat. no. 10198-018) from Invitrogen according to the manufacturer's instructions in a PC818 Program Temp. Control System from ASTEC (Fukuoka, Japan). Oligonucleotide primers used for the amplification of cDNAs for oxytocin receptor *(OTR)* were 5'-CCTTCATCGTGTGCTGGACG-3' (forward) and 5'-CTAGGAGCAGAGCACTTATG-3' (reverse); leucine-rich repeat-containing G protein-coupled receptor 4/G protein-coupled receptor 48 *(LGR4/GPR48)* were 5'-GGGAAGCT GGATGATTCGTCTTACT-3' (forward) and 5'-GAAAAGGG GAAAACAGCCTGCT-3' (reverse); trefoil factor 3 *(TFF3)* were 5'-AGAGCCTTCCCCAAGCAAACA-3' (forward) and 5'-GCAGGGGCTTGAAACACCAA-3' (reverse); brain expressed X-linked 2 *(BEX2)* were 5'-CCTTGGCCCTACCT TTGAATGT-3' (forward) and 5'-TGCTGACTGCCCGCA AACTA-3' (reverse); sarcoglycan-ε *(SGCE)* were 5'-TTCTCC AAGGTACACTCCGATCG-3' (forward) and 5'-GGCCGAT GTGATGTTTATGGC-3' (reverse); insulin-like growth factor binding protein 3 *(IGFBP3)* were 5'-ACGAGTCTCAGAGC ACAGATACCC-3' (forward) and 5'-TATCCACACACCAG CAGAAGCC-3' (reverse); and internal control glyceraldehyde-3-phosphate dehydrogenase (GAPDH) were 5'-TCCACCACC CTGTTGCTGTA-3' (forward) and 5'-ACCACAGTCCATGC CATCAC-3' (reverse), respectively. The reaction mixtures were subjected to PCR cycles of denaturation at 94˚C for 1 min, annealing at 54-59˚C for 45 sec, and extension at 72˚C for 1.5 min. RT-PCR-amplified cDNAs were visualized on 1.2% agarose gels stained with ethidium bromide and the images were captured using UVP GDS-8000 BioImaging System (Ultra Violet Products, Cambridge, UK) for further analysis using Image Pro Plus 6.0 software. The integrated optical density (IOD) = area x average density of each gene expression band was measured and normalized to that of the corresponding GAPDH expression. The RNA expression levels in the cancer cells relative to those in MKN45-GFP cells were calculated.

Western blot analysis. The cancer cells were lysed by mixing with Radio-Immunoprecipitation Assay (cat. no. R0278) buffer containing Proteinase Inhibitor Cocktail (cat. no. P8340) from Sigma. The protein amounts in the cell lysates were quantified by bicinchoninic acid protein assay kit (Pierce, Rockford, IL, USA) and mixed with electrophoresis loading buffer (50 mM Tris-HCl, 2% sodium dodecyl sulfate (SDS), 0.1% bromophenol blue, 10% glycerol, and 1 mM dithiothreitol). The prepared

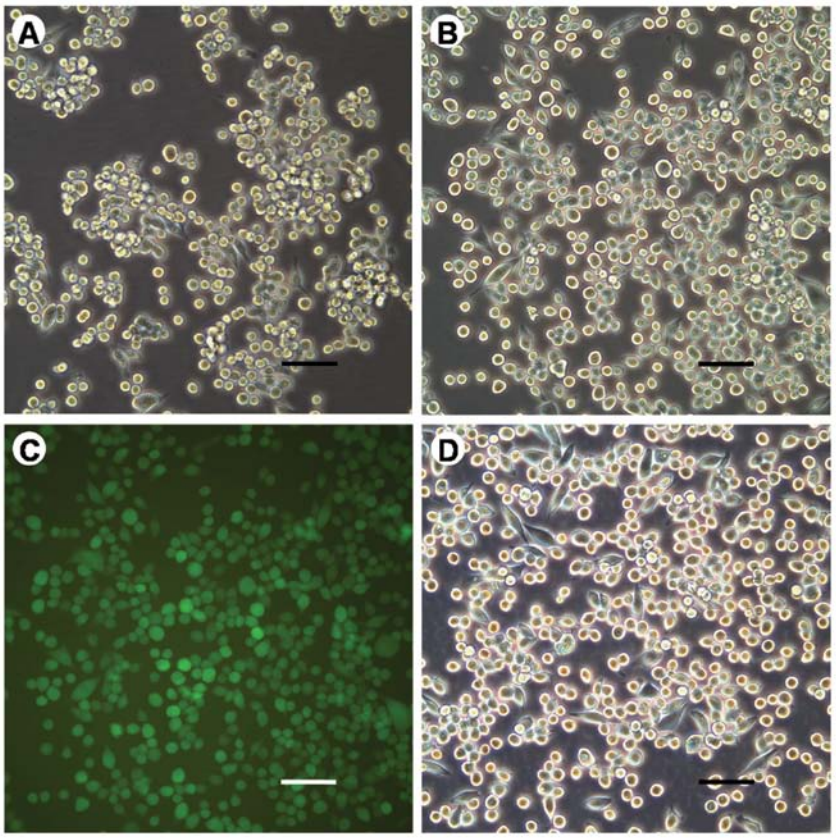

Figure 1. Morphology of MKN45-GFP and MKN45-GFP-12 cells. MKN45-GFP sublines constitutively expressing GFP proteins were established by transfection of parental MKN45 cells (A) with pEGFP-C1 plasmids. MKN45-GFP (B, bright field; C, fluorescent field) and MKN45-GFP-12 (D) cells are shown. Scale bars, 50 μm.

samples were electrophoresed on 12% SDS-polyacrylamide gel under reducing conditions. After electrophoresis, the proteins were transferred electrophoretically to the PVDF membrane (Immobilon™-P) from Millipore. The membrane was blocked with 5% skim milk for 30 min at 37˚C. After blocking, the membrane was incubated overnight at 4˚C with 1:200 diluted rabbit polyclonal antibody H-300 (cat. no. sc-28215) against human fanconi anemia complementation group A (FANCA) and C-19 (cat. no. sc-540) against metallopanstimulin 1/TTK protein kinase (MPS1/TTK) from Santa Cruz (Santa Cruz, CA, USA); and 1:500 diluted mouse monoclonal antibodies clone 294216 (cat. no. MAB2050) against human melanoma-inhibitory activity (MIA) and clone 84728 (cat. no. MAB305) against IGFBP3 from R&D Systems (Minneapolis, MN, USA) in PBS-T buffer. The membrane was washed 3 times with PBS with 0.5% Triton X-100 buffer (PBS-T) for 5 min each, and then incubated with 1:5,000 diluted horseradish peroxidase-conjugated bovine anti-rabbit IgGs (cat. no. sc-2370) from Santa Cruz or peroxidase-conjugated AffiniPure donkey anti-mouse IgGs (cat. no. 715035150) from Jackson ImmunoResearch (West Grove, PA, USA) in PBS-T buffer for 1 h at room temperature. After washing with PBS-T, the membrane was incubated with the Western Lightning™ ECL detecting reagent from Perkin Elmer (Waltham, MA, USA) and exposed to X-ray film (cat. no. 50880) from Fuji Medical (Tokyo, Japan). The images were captured by scanning exposed X-ray film using an HP Scanjet 4850 scanner (Hewlett-Packard, Palo Alto, CA, USA) and further analyzed by ImagePro Plus 6.0 software. The IOD = area x averaged density of each expressed protein band was measured and normalized to that of the corresponding GAPDH levels. The expressed protein levels in the cancer cells relative to those in MKN45-GFP cells were calculated.

Statistical analysis. Data were analyzed for significant differences using ANOVA followed by multiple comparisons with Student-Newman-Keuls test. A significant difference in the incidences of ascites and liver metastasis among the groups of nude mice was examined by using Fisher's exact test. A difference in the averaged number of tumor nodules per mouse between the two mouse groups of cancer cells inoculated was detected using Wilcoxon signed rank test. All statistical analyses were conducted using SPSS® Statistics software from SPSS Inc. (Chicago, IL, USA). A significant difference between groups was set at $p<0.05$.

Results

Stable GFP-expressing MKN45 cells. Following transfection with GFP expression plasmids using lipofectamine 2000, human gastric cancer MKN45 cell clones constitutively expressing GFP were collected. Stable GFP-expressing MKN45 cell clones were selected by G418 in culture medium and a stable GFP-expressing cell clone was isolated by the limiting dilution process. A stable MKN45 cell clone with constitutive expression of the enhanced GFP, MKN45-GFP,

Table I. Doubling time of MKN45 and MKN45-GFP sublines.

Cell line	Doubling time (day)
MKN45	1.4±0.3*
MKN45-GFP	1.7±0.1
MKN45-GFP-4	1.5±0.5
MKN45-GFP-10	1.7±0.4
MKN45-GFP-12	1.5±0.4

*Mean ± SD (n=6). No significant difference among the cells, p=0.70.

was established (Fig. 1). There was no difference in morphology between the parental MKN45 and MKN45-GFP cells (Fig. 1A and B).

Establishment of MKN45-GFP cell sublines. The MKN45-GFP cells collected after the 4th, 10th, and 12th round of 72 h-selection periods using Transwell system with Matrigel-coated porous membrane were designated as MKN45-GFP-4, MKN45-GFP-10, and MKN45-GFP-12, respectively. The cell morphologies among MKN45-GFP and MKN45-GFP cell sublines were not different from each other as shown in Fig. 1B (MKN45-GFP) and 1D (MKN45-GFP-12). Furthermore, the cell proliferation doubling times of the parental MKN45 and the established MKN45-GFP cell sublines ranged from 1.4 to 1.7 days, as shown in Table I, and were not significantly different from each other (p=0.70).

MKN45-GFP cell sublines with different in vitro invasion abilities. The three established MKN45-GFP sublines exhibited different invasive abilities in an increasing tendency, sequentially as MKN45-GFP, MKN45-GFP-4, MKN45-GFP-10 and MKN45-GFP-12. Fig. 2A-E shows representative images of hematoxylin-stained invaded cells on the surface of the porous membrane of the lower chamber of Transwell cultures. There was no difference in invasion ability between the parental MKN45 and MKN45-GFP cells, whereas significantly more MKN45-GFP-10 and MKN45-GFP-12 cells invaded through the membrane onto the other side of the membrane compared to MKN45 and MKN45-GFP cells. In comparison to that of MKN45-GFP, the invasion ability was significantly increased by 2-, 6-, and 6-fold for MKN45-GFP-4, MKN45-GFP-10 and MKN45-GFP-12 cells, respectively, as shown in Fig. 2F.

Incidences of ascites caused by MKN45-GFP and MKN45-GFP-12 cells in nude mice. The incidences of ascites in the MKN45-GFP and MKN45-GFP-12 cells inoculated nude mice were monitored as an index of tumorigenic aggressiveness and tumor burden caused by the cells. As the data summarized in Table II show, MKN45-GFP-12 cells caused a significant on-set of ascites on week 4 after the inoculation, which is one week earlier than that caused by MKN45-GFP cells. The higher incidence of ascites at week 4 caused by MKN45-GFP-12 indicated a higher tumorigenic aggressiveness of MKN45-GFP-12 than MKN45-GFP cells.

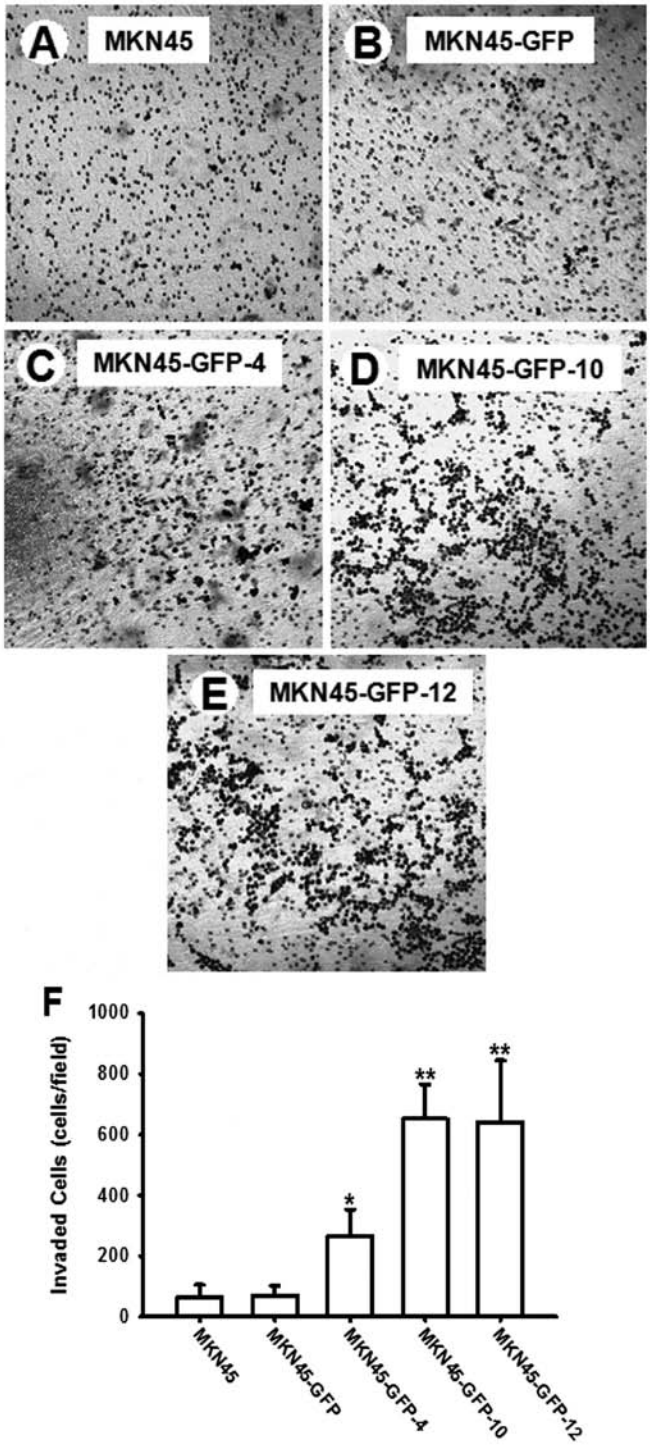

Figure 2. Invasion ability of MKN45 and MKN45-GFP cell sublines. (A-E) Invaded MKN45 and MKN45-GFP cells were fixed with 10% formaldehyde followed by hematoxylin staining as shown (magnification, x100). (F) The number of invaded cells on the bottom surface of the Transwell® membrane was counted for each cell subline. MKN45-GFP-4, MKN45-GFP-10, and MKN45-GFP-12 cells exhibited a 2-, 6-, and 6-fold increase, respectively, in the invasion ability relative to that of MKN45-GFP (*$p<0.05$), n=4. Differential invasion abilities were also observed in MKN45-GFP-4 vs. MKN45-GFP-10 and MKN45-GFP vs. MKN45-GFP-12 cells.

Orthotopic tumorigenesis and liver metastasis of MKN45-GFP and MKN45-GFP-12 cells in nude mice. Adult male nude mice intraperitoneally inoculated with MNK45-GFP or MKN45-GFP-12 cells were observed for intraperitoneal

Table II. Incidence of ascites in the nude mice intraperitoneally inoculated with the cancer cells.

	Week 2*	Week 3	Week 4	Week 5
MKN45-GFP	0/7	1/7	1/7	6/7
MKN45-GFP-12	0/7	1/7	6/7**	6/7

*Time when animals were sacrificed following inoculation. **p=0.015 vs. MKN45-GFP, Fisher's exact test.

Table III. Incidence of liver metastasis in the nude mice intraperitoneally inoculated with the cancer cells.

	No metastasis	Metastasis
MKN45-GFP	33/35 (94%)	2/35 (6%)
MKN45-GFP-12	27/35 (77%)	8/35 (23%)*

*p=0.042 vs. MKN45-GFP, Fisher's exact test.

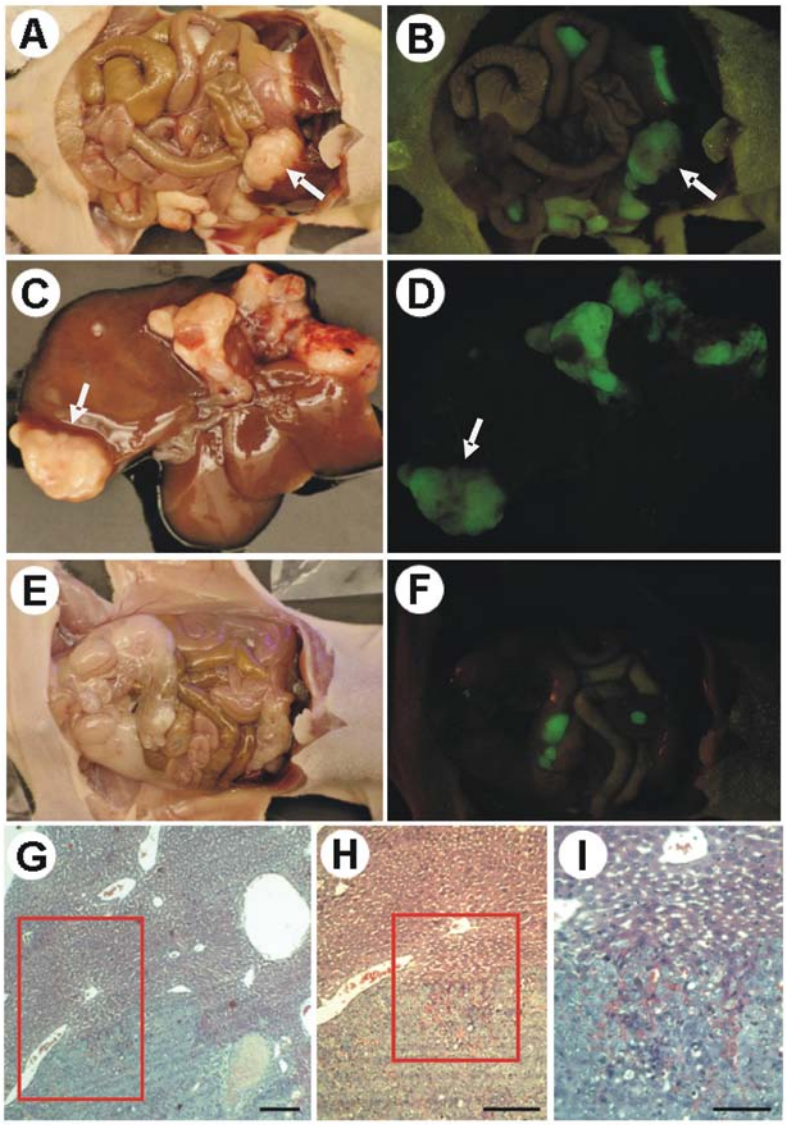

Figure 3. *In vivo* orthotopic growths of MKN45-GFP and MKN45-GFP-12 tumors in nude mice. MKN45-GFP-12 tumors orthotopically grew in the intraperitoneally disseminated condition inside the peritonea of the nude mice. A representative mouse after laparotomy with the growing tumors was visualized in bright (A) and fluorescent (B) fields. As the arrows indicate, the mouse liver with metastasized MKN45-GFP-12 tumors was dissected and observed in bright (C) and fluorescent (D) fields. Orthotopically growing MKN45-GFP tumors in a nude mouse are shown in bright (E) and fluorescent (F) fields. A hematoxylin-eosin stained tissue section of a nude mouse liver invaded by an MKN45-GFP-12 tumor is shown in different magnifications in (G-I). Scale bars, 200 μm for (G) and (H), and 50 μm for (I).

tumorigenesis and the numbers of tumor nodules were counted by visualizing the GFP-expressing tumors using a fluorescence imaging system. The orthotopic intraperitoneal inoculation of gastric cancer cells of diffuse type in mice is to mimic the dissemination and metastasis conditions of the cancer cells in the peritoneum of gastric cancer patients. After the inoculation, MKN45-GFP-12 tumor cells grew inside the peritoneal cavity and metastasized to and grew in the mouse

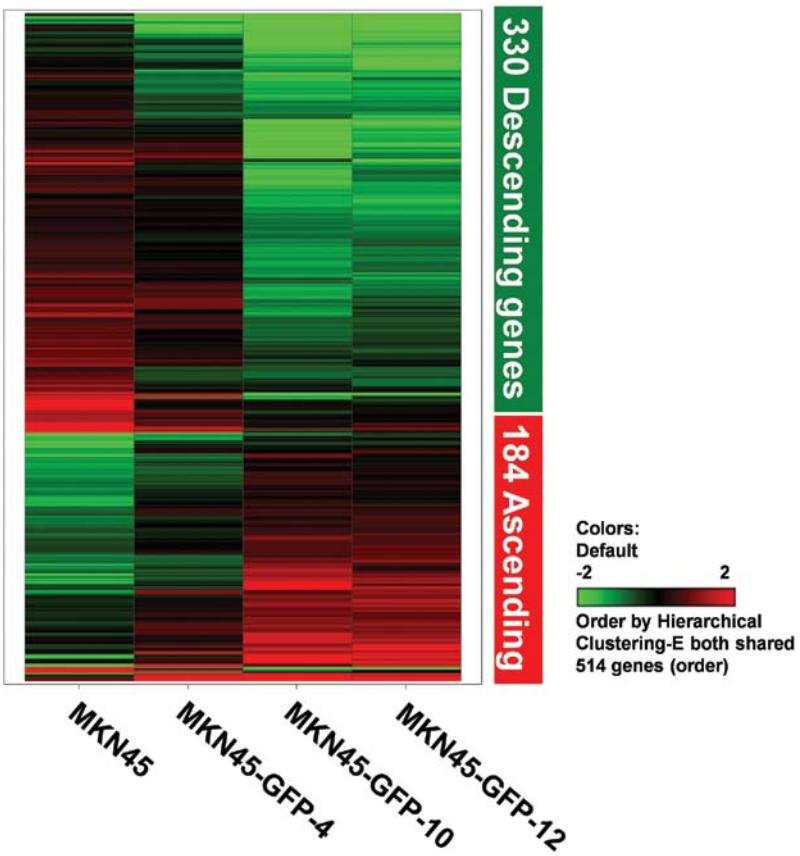

Figure 4. Hierarchical clustering analysis of gene profiles of the MKN45 cell sublines. Four MKN45 sublines with varying invasion abilities were microarray analyzed, and the gene expression trends calculated against that of the control subline MKN45-GFP were determined. All genes that shared a similar trend of ascending or descending property were clustered, respectively, and 330 descending and 184 ascending genes were identified.

liver. Representative images of the intraperitoneally disseminated growing MKN45-GFP-12 tumors in a nude mouse after laparotomy in bright and fluorescent fields are shown in Fig. 3A and B, respectively. Growing MKN45-GFP-12 tumors that invaded into the mouse liver are shown in Fig. 3C (bright field) and D (fluorescent field). MKN45-GFP cells also grew into tumors in the mouse peritoneum as shown in Fig. 3E (bright field) and F (fluorescent field). On Day 14 after the cancer cell inoculation, we observed that MKN45-GFP cells caused 14-25 (median 17; mean 18; n=7) intraperitoneally orthotopic growing tumors, whereas MKN45-GFP-12 cells caused 10-40 (median 25; mean 24; n=7) intraperitoneally orthotopic growing tumors in the laparotomized nude mice. The number of intraperitoneal tumor nodules caused by the orthotopic inoculation was compared and MKN45-GFP-12 cells were found to cause more, though not statistically significant (p=0.128), intraperitoneally disseminated growing tumors in the nude mice. Furthermore, both intraperitoneally inoculated MKN45-GFP and MKN45-GFP-12 cells caused metastatic tumor growth in the nude mouse livers during the observation period (Fig. 3G-I). MKN45-GFP-12 cells metastasized to the mouse liver and established metastatic growth in more nude mouse livers (p=0.042) than MKN45-GFP cells as detailed in the liver metastasis incidence summary in Table III. The results showed that MKN45-GFP-12 cells exhibited a higher metastasizing potential *in vivo* than MKN45-GFP cells.

cDNA microarray analyses of genes in MKN45-GFP cell sublines. Total RNAs from the established MKN45-GFP and the selected MKN45-GFP-4, MKN45-GFP-10, and MKN45-GFP-12 cells were cDNA microarray analyzed. The gene expression levels and patterns of MKN45-GFP-4, MKN45-GFP-10, and MKN45-GFP-12 cells were compared in relation to those of the MKN45-GFP cells (GEO accession number GSE33570). We used the PvalueLogRatio method to sieve out significant spots of whole microarray analysis. PvalueLogRatio gives the statistical significance on the log ratio for each spot between experimental and control signals. In order to focus on the desired data, we setup the criteria for removal steps and filtering procedure to identify positive or negative expression-correlated 514 genes (184 ascending and 330 descending genes) of the examined genes by hierarchical clustering calculation. We found that only <3% of all genes may be involved in human gastric cancer invasion and metastasis. Fig. 4 displays a hierarchical clustering analysis image with 514 genes (accounting for 2.75% of the total number of 18,716 genes examined) from significant expression levels by using the selection criteria described above, which share a similar tendency containing 184 ascending (positively correlated with invasiveness) and 330 descending genes (negatively correlated with invasiveness). The expression levels were pseudo-color encoded showing the descending and ascending expression levels of genes in the MKN45-GFP cell sublines. Based on the hierarchical clustering analyses, the expression patterns of

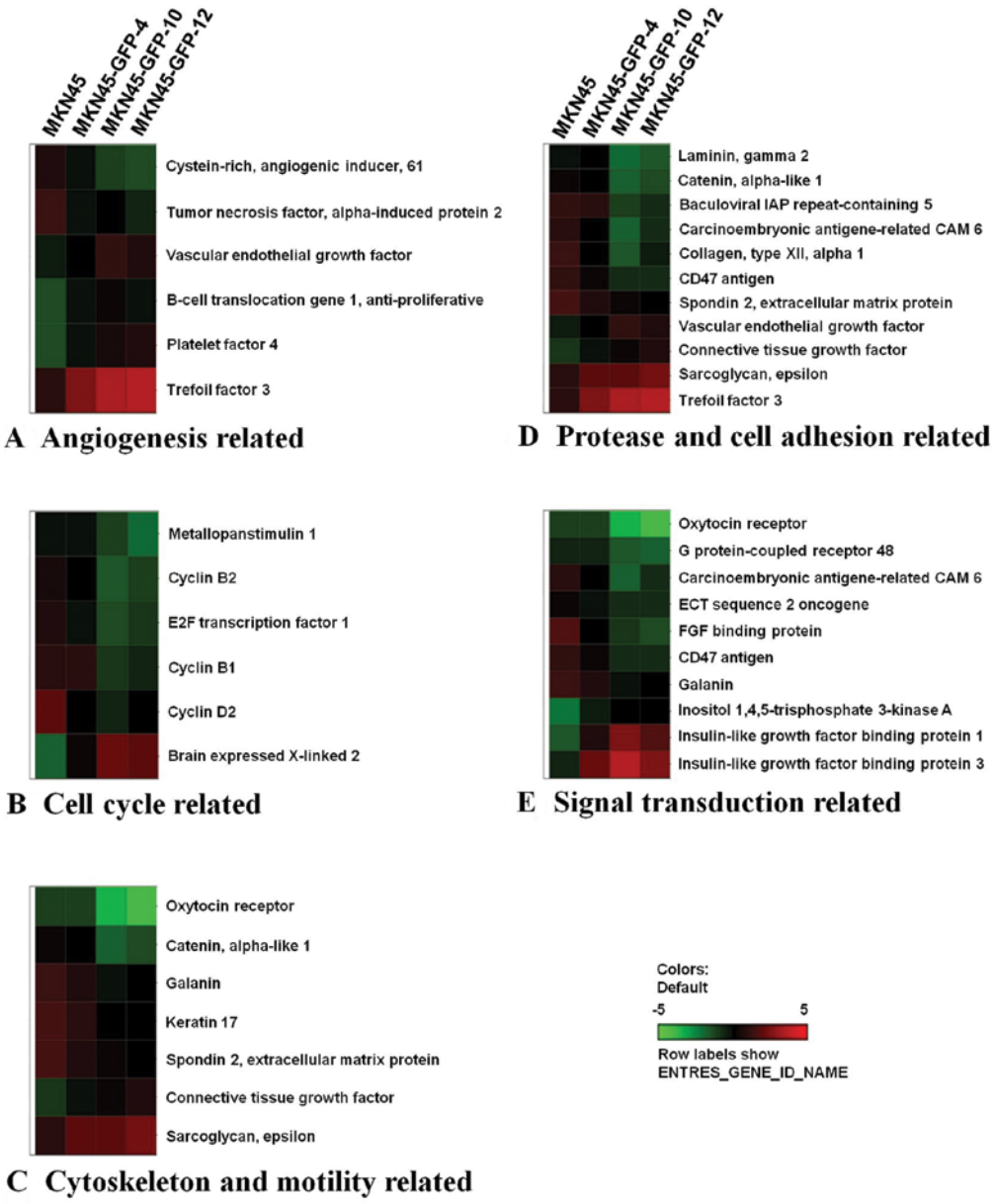

Figure 5. Functional grouping of invasion/metastasis-associated genes. The genes after the hierarchical clustering analysis were grouped into categories on the basis of their cellular functions. Representative genes were listed in five functional groups as: (A) angiogenesis related genes, (B) cell cycle regulation related genes, (C) cytoskeleton and motility related genes, (D) protease and cell adhesion related genes, and (E) signal transduction related genes. Genes with multiple cellular functions were included in more than one functional group.

these 514 genes were subjected to regulating tendency selection processes.

The 514 genes identified in the hierarchical clustering analysis were further categorized into groups such as angiogenesis-related genes, cell cycle regulators, cytoskeleton and motility molecules, protease and adhesion proteins, and signal transduction molecules, based on known molecular and biological functions associated with tumor progression. A total of 133 genes were found to be associated with these biological functions and 30 of them are shown in Fig. 5 and Table IV. The 5 selective groups were (A) angiogenesis-related genes such as angiogenic inducer *Cyr61* and vascular endothelial growth factor; (B) cell cycle regulators such as *MPS1/TTK* and cyclin B2; (C) cytoskeleton and motility molecules such as *OTR* and catenin α-like 1; (D) protease and adhesion molecules such as laminin γ 2 and collagen type XII α 1, and (E) signal transduction molecules such as *LGR4/GPR48 and* heparin-binding growth factor binding protein. Genes associated with multiple biological functions were included in the corresponding categorized functional groups accordingly. A number of genes that have not been previously reported to correlate with cancer progression or tumor metastasis were also identified and are listed in Table V. The levels of these genes differed more than two-fold between highly metastatic and parental cells, indicating that these genes may play significant roles in gastric cancer metastasis.

mRNA transcript levels in MKN45-GFP cell sublines. Several putative tumor metastasis-associated genes were further examined by using RT-PCR analysis. Four genes,

Table IV. Genes of known functions differentially expressed between parental and highly metastatic MKN45 cell lines.

Probe name	Accession no.	Sequence homology (GenBank/EMBL)	Gene symbol	Chromosome location	$Log_2[E_{12}/E_p]$
		Angiogenesis related genes			
A_23_P257296	NM_003226	Trefoil factor 3	TFF3	21q22.3	2.74
A_23_P132987	NM_002619	Platelet factor 4	PF4	4q12-q21	2.06
A_23_P387668	NM_003376	Vascular endothelial growth factor	VEGFA	6p12	1.40
A_23_P87564	NM_001731	B-cell translocation gene 1, anti-proliferative	BTG1	12q22	1.24
A_23_P421423	NM_006291	Tumor necrosis factor, α-induced protein 2	TNFAIP2	14q32	-1.76
A_23_P46429	NM_001554	Cystein-rich, angiogenic inducer, 61	CYR61	1p31-p22	-2.12
		Cell cycle regulation related genes			
A_23_P22735	NM_032621	Brain expressed X-linked 2	BEX2	Xq22	3.99
A_23_P122197	NM_031966	Cyclin B1	CCNB1	5q12	-1.56
A_23_P80032	NM_005225	E2F transcription factor	E2F1	20q11.2	-1.66
A_23_P65757	NM_004701	Cyclin B2	CCNB2	15q22.2	-1.78
A_23_P259586	NM_003318	Metallopanstimulin 1	TTK	6q13-q21	-1.85
A_23_P139881	NM_001759	Cyclin D2	CCND2	12p13	-2.33
		Cytoskeleton and motility related genes			
A_23_P19663	NM_001901	Connective tissue growth factor	CTGF	6q23.1	1.56
A_23_P254626	NM_003919	Sarcoglycan, epsilon	SGCE	7q21-q22	1.46
A_23_P374844	NM_015973	Galanin	GAL	11q13.3	-1.52
A_23_P121533	NM_012445	Spondin 2, extracellular matrix protein	SPON2	4p16.3	-1.57
A_23_P96149	NM_000422	Keratin 17	KRT17	17q12-q21	-1.59
A_23_P157795	NM_003798	Catenin, α-like 1	CTNNAL1	9q31.2	-2.14
A_23_P132619	NM_000916	Oxytocin receptor	OXTR	3p25	-2.90
		Protease and cell adhesion related genes			
A_23_P257296	NM_003226	Trefoil factor 3	TFF3	21q22.3	2.74
A_23_P19663	NM_001901	Connective tissue growth factor	CTGF	6q23.1	1.56
A_23_P254626	NM_003919	Sarcoglycan, epsilon	SGCE	7q21-q22	1.46
A_23_P387668	NM_003376	Vascular endothelial growth factor	VEGFA	6p12	1.40
A_23_P121533	NM_012445	Spondin 2, extracellular matrix protein	SPON2	4p16.3	-1.57
A_23_P6935	NM_001777	CD47 antigen	CD47	3q13.1-q13.2	-1.89
A_23_P201636	NM_005562	Laminin, gamma 2	LAMC2	1q25-q31	-2.00
A_23_P118815	NM_001168	Baculoviral IAP repeat-containing 5	BIRC5	17q25	-2.12
A_23_P157795	NM_003798	Catenin, α-like 1	CTNNAL1	9q31.2	-2.14
A_23_P218441	NM_002483	Carcinoembryonic antigene-related CAM 6	CEACAM6	19q13.2	-2.61
A_23_P214168	NM_004370	Collagen, type XII, α 1	COL12A1	6q12-q13	-2.74

Table IV. Continued.

Probe name	Accession no.	Sequence homology (GenBank/EMBL)	Gene symbol	Chromosome location	$Log_2[E_{12}/E_p]$
		Signal transduction related genes			
A_23_P42869	NM_000596	Insulin-like growth factor binding protein 1	IGFBP1	7p13-p12	4.19
A_23_P215634	NM_000598	Insulin-like growth factor binding protein 3	IGFBP3	7p13-p12	4.10
A_23_P4714	NM_006533	Melanoma inhibitory activity	MIA	19q13.32-q13.33	2.73
A_23_P65918	NM_002220	Inositol 1,4,5-trisphosphate 3-kinase A	ITPKA	15q14-q21	2.44
A_23_P9571	NM_018098	ECT sequence 2 oncogene	ECT2	3q26.1-q26.2	-1.13
A_23_P203767	NM_018490	G protein-coupled receptor 48	LGR4	11p14-p13	-1.35
A_23_P206441	NM_000135	Fanconi anemia, complementation group A	FANCA	16q24.3	-1.38
A_23_P374844	NM_015973	Galanin	GAL	11q13.3	-1.52
A_23_P6935	NM_001777	CD47 antigen	CD47	3q13.1-q13.2	-1.89
A_23_P218441	NM_002483	Carcinoembryonic antigene-related CAM 6	CEACAM6	19q13.2	-2.61
A_23_P132619	NM_000916	Oxytocin receptor	OXTR	3p25	-2.90
A_23_P30126	NM_005130	FGF binding protein	FGFBP1	4p16-p15	-3.20

$Log_2[E_{12}/E_p]$ corresponds to 2 logarithm of mean expression ration of MKN45-GFP-12 (E_{12}) to MKN45 parental cell line (E_p).

Table V. Novel genes of unknown functions differentially expressed between parental and highly metastatic MKN45 cell lines.

Probe name	Accession no.	Sequence homology (GenBank/EMBL)	Gene symbol	Chromosome location	$Log_2[E_{12}/E_p]$
A_23_P209360	NM_052920	Kelch-like 29	KLHL29	2p24.1	3.26
A_23_P20876	NM_152422	Protein tyrosine phosphatase domain containing 1	PTPDC1	9q22.32	2.51
A_23_P83339	NM_145051	Ring finger protein 183	RNF183	9q32	2.14
A_23_P108823	NM_145739	Oxysterol binding protein-like 6	OSBPL6	2q32.1	1.92
A_23_P154740	NM_018474	Polo-like kinase 1 substrate 1	PLK1S1	20p11.23	1.80
A_23_P79302	NM_177964	LY6/PLAUR domain containing 6B	LYPD6B	2q23.2	1.44
A_23_P52727	NM_182964	Neuron navigator 2	NAV2	11p15.1	-1.49
A_23_P51966	NM_003035	SCL/TAL1 interrupting locus	STIL	1q32; 1p32	-1.55
A_23_P379778	NM_017594	DIRAS family, GTP-binding RAS-like 2	DIRAS2	9q22.2	-1.56
A_23_P69179	NM_018192	Leprecan-like 1	LEPREL1	3q28	-1.57
A_23_P340909	NM_145061	Spindle and kinetochore associated complex subunit 3	SKA3	13q12.11	-1.66
A_23_P118582	NM_013290	PSMC3 interacting protein	PSMC3IP	17q21.2	-1.70
A_23_P48835	NM_138555	Kinesin family member 23	KIF23	15q23	-1.80
A_23_P166526	NM_015653	RIB43A domain with coiled-coils 2	RIBC2	22q13.31	-1.90
A_23_P80718	NM_144642	Synaptoporin	SYNPR	3p14.2	-1.92
A_23_P49878	NM_019013	Family with sequence similarity 64, member A	FAM64A	17p13.2	-1.93
A_23_P323751	NM_030919	Family with sequence similarity 83, member D	FAM83D	20q11.22-q12	-1.95
A_23_P42811	NM_176813	Anterior gradient homolog 3	AGR3	7p21.1	-2.06
A_23_P388812	NM_152515	Cytoskeleton associated protein 2-like	CKAP2L	2q13	-2.07

Table V. Continued.

Probe name	Accession no.	Sequence homology (GenBank/EMBL)	Gene symbol	Chromosome location	$Log_2[E_{12}/E_p]$
A_23_P25964	NM_000153	Galactosylceramidase	GALC	14q31	-2.16
A_23_P355525	NM_173497	HECT domain containing 2	HECTD2	10q23.32	-2.39
A_23_P250853	N/A	SM3A_HUMAN (Q14563) Semaphorin 3A precursor (Semaphorin III) (Sema III), partial (8%)	THC2052903	N/A	-2.41
A_23_P35995	NM_024769	Adipocyte-specific adhesion molecule	ASAM	11q24.1	-2.49
A_23_P3302	NM_018365	Meiosis-specific nuclear structural 1	MNS1	15q21.3	-2.50
A_23_P217785	NM_016500	Chromosome X open reading frame 26	CXorf26	Xq13.3	-2.54
A_23_P130027	NM_017957	Epsin 3	EPN3	17q21.33	-2.60
A_23_P301360	NM_152412	Zinc finger protein 572	ZNF572	8q24.13	-2.62
A_23_P254842	NM_012080	Haloacid dehalogenase-like hydrolase domain containing 1	HDHD1	Xp22.32	-2.68
A_23_P329254	NM_153032	Archaelysin family metallopeptidase 2 pseudogene 1	AMZ2P1	17q24.1	-2.69
A_23_P35871	NM_024680	E2F transcription factor 8	E2F8	11p15.1	-2.75
A_23_P154279	NM_032309	Coiled-coil-helix-coiled-coil-helix domain containing 5	CHCHD5	2q13	-3.01
A_23_P252432	NM_004617	Transmembrane 4 L six family member 4	TM4SF4	3q25	-3.06
A_23_P75915	NM_024557	Resistance to inhibitors of cholinesterase 3 homolog (C. elegans)	RIC3	11p15.4	-3.06
A_23_P252388	NM_024867	Sperm flagellar 2	SPEF2	5p13.2	-3.20
A_23_P396765	NM_173582	Phosphoglucomutase 2-like 1	PGM2L1	11q13.4	-3.41
A_23_P139604	NM_003805	CASP2 and RIPK1 domain containing adaptor with death domain	CRADD	12q21.33-q23.1	-4.71

$Log_2[E_{12}/E_p]$ corresponds to 2 logarithm of mean expression ration of MKN45-GFP-12 (E_{12}) to MKN45 parental cell line (E_p).

TFF3, *BEX2*, *SGCE* and *IGFBP3*, positively correlated with the invasion ability, and two genes, *OTR* and *LGR4*/*GPR48*, negatively correlated with the invasion ability of the gastric cancer MKN45-GFP cell sublines, were RT-PCR analyzed. The housekeeping gene GAPDH was selected as the internal control. Results showed that all four examined genes *TFF3*, *BEX2*, *SGCE*, and *IGFBP3* exhibited an increasing order of the mRNA transcript levels from MKN45-GFP, MKN45-GFP-4, MKN45-GFP-10, to MKN45-GFP-12 cells. On the other hand, mRNA transcript levels of the two genes *OTR* and *LGR4*/*GPR48* were in a decreasing order in these MKN45-GFP cell sublines in relation to their invasion ability (Fig. 6). Results of the RT-PCR analyses on these selective genes were consistent with those from the cDNA microarray analyses.

Protein expression levels in MKN45-GFP cell sublines. The expression levels of several proteins of the microarray-identified genes were also examined using western blot analysis. FANCA, MPS1/TTK, MIA, and IGFBP3 protein levels in the MKN45-GFP cell sublines were analyzed in triplicates. FANCA and MPS1/TTK protein levels were downregulated with the increase of the invasive potentials of the MKN45-GFP cell sublines. By contrast, the protein levels of (precursor and/or mature) MIA and IGFBP3 were upregulated with the increase of the invasive potentials of the MKN45-GFP cell sublines (Fig. 7). Both the mRNA transcript and protein expression levels of the *IGFBP3* gene were positively correlated with the invasive abilities of the MKN45-GFP cell sublines. The results demonstrated that the expression levels of these proteins examined were consistent with those from the cDNA microarray analyses.

Discussion

It is well known that differential expression of multiple genes and dynamic interactions of a number of cellular proteins are

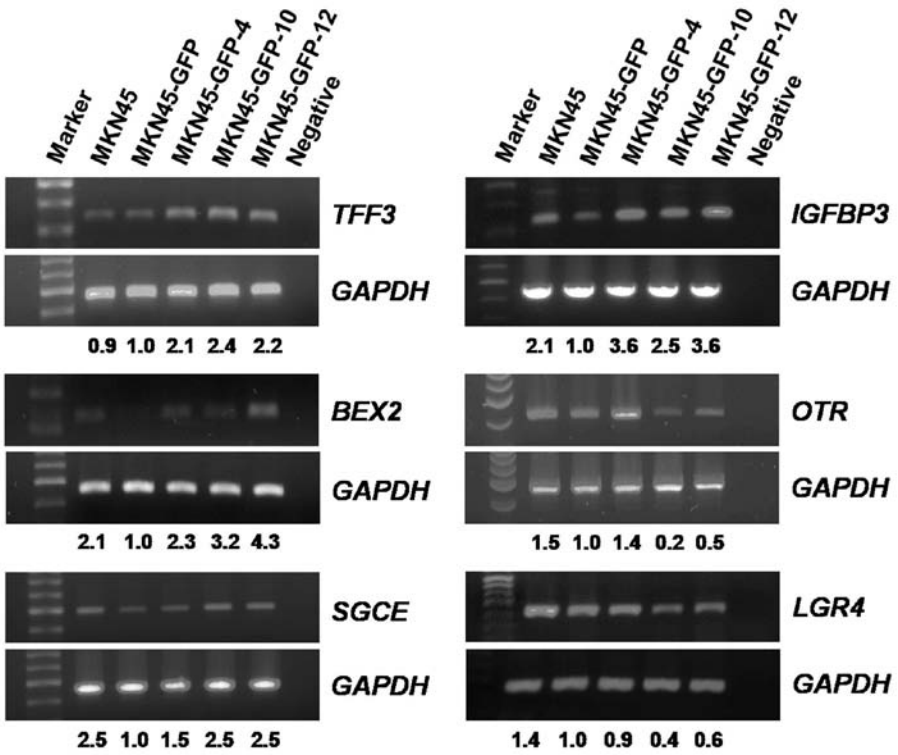

Figure 6. Reverse transcriptase PCR analysis of mRNA levels in MKN45-GFP cell sublines. Four genes (*TFF3, BEX2, SGCE, IGFBP3*) with ascending mRNA levels and two genes (*OTR, LGR4/GPR48*) with descending mRNA levels were analyzed. The level of GAPDH mRNA was used as the internal control for normalization. The relative mRNA levels of the genes compared to that of MKN45-GFP were indicated accordingly. (*TFF3*, trefoil factor 3; *BEX2*, brain expressed X-linked 2; *SGCE*, sarcoglycan, epsilon; *IGFBP3*, insulin-like growth factor binding protein 3; *OTR*, oxytocin receptor; *LGR4/GPR48*, leucine-rich repeat-containing G protein-coupled receptor 4/G protein-coupled receptor 48).

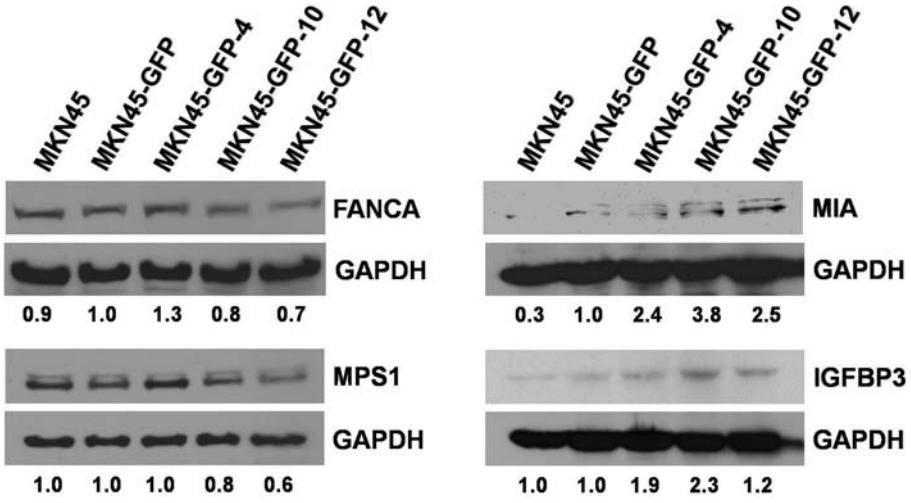

Figure 7. Correlated expression levels of proteins in MKN45-GFP and MKN45-GFP cell sublines. The expressed protein levels of four genes with descending (*FANCA, MPS1*) and ascending (*MIA, IGFBP3*) mRNA expression trends, respectively, in the MKN45-GFP sublines in relation to the invasiveness were analyzed. The protein level of GAPDH was used as internal control for normalization of the protein expression levels. The relative protein expression levels compared to that of MKN45-GFP were image-analyzed and indicated in numbers accordingly. Each experiment was carried out in triplicates. (FANCA, fanconi anemia complementation group A; MPS1/TTK protein kinase, metallopanstimulin 1; MIA, melanoma-inhibitory activity; IGFBP3, insulin-like growth factor binding protein 3).

involved in the multiple progressive steps of cancer metastasis including gastric cancer. cDNA microarray has been applied to explore the expression profiles of a massive number of genes between testing cancer samples. In the present study, we used cDNA microarray to identify gastric cancer invasion/metastasis-associated genes on a genome-wide scale in human gastric cancer sublines that have demonstrated different metastatic abilities. As the poorly differentiated diffuse type gastric cancer remains an unmet medical need, a gastric cancer cell line of diffuse type MKN45, originally isolated from a

poorly differentiated adenocarcinoma of a patient's stomach (33,34), was used as the model cell. By taking advantage of the fluorescence-emitting ability of GFP, we established an MKN45 cell line constitutively expressing GFP which can be visualized, and applied it to select the MKN45-GFP sublines with differential invasion abilities by using the Transwell system. Genes in relation to the invasiveness of these sublines were identified using cDNA microarray analysis and verified by RT-PCR and western blot analyses. Furthermore, the invasiveness of the highly invasive subline MKN45-GFP-12 was *in vivo* demonstrated by the incidence of ascites and organ invasive abilities in nude mice. Meanwhile, we observed that a number of the identified genes are also related to angiogenesis, cell cycle, cytoskeleton and motility, protease and cell adhesion, and signal transduction, which are cellular events known to be associated with invasion and tumor metastasis (39). Accordingly, a number of novel genes without previously known cancer-related biological activities were also identified in relation to gastric tumor metastasis in the present study.

Systemically analyzed using genomic microarray technologies and biological activity assays, genes putatively associated with tumor cell invasion and metastasis have been identified in various human cancer cells, including gastric cancer cells. Many studies utilized microarray technologies to discover genes specifically associated with tumor invasion and metastasis. Hippo *et al* observed a number of differentially expressed genes by using a set of human gastric scirrhous cancer cells prone to peritoneal and lymph node metastasis in nude mice (23). Although the array-based oligonucleotide hybridization method is a powerful tool for identifying potential genes associated with tumor metastasis, the genes reported in these above-mentioned studies are different from each other. The intrinsic heterogeneity of the cancer cell populations in patient tumor tissues likely mixed with normal stromal and/or vascular cells may contribute to these observed discrepancies in the gene expression profiles (40). Herein we used a human gastric cancer cell line of diffuse type *in vitro* to normalize and minimize the potentially existing heterogeneity in order to identify human gastric tumor metastasis-associated genes.

Chronic infection of *Helicobacter P.* has been proven to be an important etiologic factor of gastric cancer (41) and accounts for 18% of all cancers caused by infections (42). Helicobacter infection has been found to be associated with β-catenin, MMP-1, ERK (p38), EGFR, AP-1, Shh, CDX2, E-cadherin (CDH1), p16, APC, MLH1, COX2, IL-1, IL-6, IL-10, CTLR4, BCL-2, FOXP1 and p53 (43), and IL-8, ras family and Ras p21 are involved in the TNFα/NF-κB/IκB-mediated gastric tumorigenesis (44). Helicobacter colonization is usually asymptomatic and gastric tumorigenesis occurs only in a subset of individuals depending on the host response and genetic variation of the bacteria. The infection alone could not attribute entirely to the gastric tumorigenesis as the clinically observed human gastric cancers are genetically and histologically diversifying (43,45). Although several studies reported that Helicobacter infection increases tumor invasiveness and metastasis via multiple molecular pathways (46-50), in the present study we did not find significant changes in the expressions of these mentioned genes and/or the genes in the TNFα/NF-κB/IκB-mediated signaling pathways (43,44). Therefore, the results suggest that the genes identified in the present study are not Helicobacter infection-related and are thus directly correlated to the metastatic abilities of human gastric cancer tumors.

GFP has been utilized as a reporter molecule and has been widely applied *in vitro* and *in vivo* to visualize the developmental processes of tumors, including primary and metastatic tumor growths, tumor cell metastases, tumor angiogenesis, and interactions between tumor and the host microenvironment (38,51-54). Chu *et al* established a set of human lung cancer cells with differential invasive abilities (35), Chen *et al* identified a number of genes associated with human lung cancer metastasis (55), and Chen *et al* demonstrated a significant clinical association for some of these identified genes (56). Accordingly, we took advantage of the fluorescence-emitting GFP and established the human GFP-expressing MKN45 sublines with differential invasive abilities in the present study. The morphology and proliferation rates were not different from each other among these established MKN45-GFP sublines including the parental MKN45 cells. One of the important advantages is that we are able to monitor the tumor growth and peritoneal dissemination in individual nude mice without laparotomy. The appropriate timing for animal euthanization can then easily be determined and therefore the number of animals used in a study can be reduced. The identification of the genes previously known with biological activities related to tumor progression and metastasis suggests the validity of the approach utilized in this study. The observations indicate that the genes differentially expressed among these sublines are likely to be associated with their invasive and, thus, metastatic abilities.

In the present study, 184 and 330 genes were found positively and negatively expressed, respectively, with regard to the increasing order of the invasive abilities of these model cell sublines. The identified genes are likely to be associated with cancer progression and/or tumor metastasis. They are found to be associated with the biological activities pertaining to tumor metastasis such as angiogenesis-, cell cycle regulation-, cytoskeleton and motility-, protease and cell adhesion-, and signal transduction-related genes as shown in Fig. 5 and Table IV. Angiogenesis is one of the essential steps of tumor growth and metastasis (39). Proteins of the trefoil factor family genes may induce tumor vascularity and be associated with tumor metastatic phenotype and recurrence in human gastric cancer (57). Trefoil factor 3 (TFF3) is connected with multiple oncogenic pathways such as COX2 and EGFR and participates in the blood vessel formation during tumor progression (58). IGFBP3 is a protein of multi-functions. IGFBP3 induces IGF-independent anti-angiogenic effects and exerts tumor suppressive effects against prostate cancer (59) and non-small cell lung cancer (60), whereas its overexpression is associated with the increasing metastatic ability of well-differentiated pancreatic endocrine tumors (61). We report here that IGFBP3 expression is positively correlated with the invasive ability of human gastric cancer cells suggesting that IGFBP3 is involved in gastric cancer metastasis. In agreement with a previous study (62), we found that vascular endothelial growth factor (VEGF) genes were positively regulated in accordance with the development of tumor invasiveness. Overexpression of B-cell translocation gene 1 (BTG1) increases tube formation and migration of the endothelial cells (63). Accordingly, we

observed that BTG1 is upregulated during the development of human gastric cancer cell invasiveness. Further studies are required to explore the pathological roles of these angiogenesis-related genes during gastric tumor progression.

During cell cycle progression, MPS1/TTK is a protein kinase and is involved in the regulation of centrosomal control of cytokinesis in the mitotic checkpoint process (64). MPS1/TTK kinase affects the chromosomal stabilities in the M phase of the cell cycles in zebra fish and mammalian cells (65,66). Chromosomal instability may induce changes in the cellular functions and thus increase the invasive and metastatic abilities of tumor cells (67). In accordance with the implications of these observations, we found that MPS1/TTK expression was downregulated in the invasive cell sublines. BEX2 participates in G1 phase regulation during cell cycle progression and its over-expression protects breast cancer cells against mitochondrial apoptosis (68). We herein observed that upregulation of BEX2 was associated with the development of the invasion and metastasic abilities of gastric tumor cells.

Cellular cytoskeleton and motility also play important roles in tumor cell metastasis. Connective tissue growth factor (CTGF), whose transcript levels were moderately increased, as shown in the present study, modulates the motility of human breast cancer cells through activation of the ERK1/2 signaling pathway (69). Catenin-α is anti-metastatic in human squamous carcinoma and breast cancer by forming a complex with E-cadherin and thus enhancing the cell-cell adhesion (70,71). In agreement with these observations, catenin-α was downregulated in the invasive cell sublines in this study. Oxytocin receptor was found in the smooth muscles of the gastric/intestinal system and mediates gastric motility (72). A previous study showed that oxytocin inhibited ovarian carcinoma cell metastasis *in vitro* and *in vivo* (73). Furthermore, we observed that oxytocin receptors are downregulated in the highly metastatic gastric cancer cell sublines. The results suggest that the oxytocin/oxytocin receptor system may play a significant role in gastric cancer metastasis.

Proteases and adhesion proteins play key roles in gastric tumor metastasis. The ability of tumor cells to detach from a primary tumor tissue and degradation of the extracellular matrix and basement membrane structures are associated with the progress of tumor cell invasion and metastasis. TFF3 modulates E-cadherin/catenin-mediated cell-cell contact and increases cell motility in cancer progression (74). We found that TFF3 was upregulated in the gastric cancer cells with high invasive ability. Involvement of SGCE in adhesion activity has been reported to inhibit the invasion of colorectal tumors (75). Contrary to that observed in colorectal tumors, SGCE expression was positively correlated with the gastric cancer cell invasion ability shown in the present study. Laminin family proteins involved in the cell-laminin interactions are related to tumor angiogenesis, invasion and metastasis (76). We found that laminin-γ was downregulated in the gastric cancer cells of high invasiveness. Collagen XII is an adhesion protein reported to have critical roles in the interactions between cancer cells and bone marrow, in cell adhesion, and in cell motility and is thus involved in the bone metastasis of prostate cancer (77). In gastric cancer cells, we observed that collagen XII expression is inversely correlated with cancer cell invasion ability.

Cellular and subcellular signaling pathways regulate multiple and complex cellular activities, including tumor cell proliferation, invasion and metastasis. IGFBP3 plays significant roles in tumor cell proliferation, invasion and metastasis in different human cancer diseases. Compared to the primary melanoma cells, IGFBP3 was overexpressed in the metastatic melanoma cells and may serve as a biomarker in the early diagnosis of melanoma (78). On the other hand, Torng *et al* reported that IGFBP3 plays a major role as an invasion-metastasis suppressor via an insulin growth factor-independent pathway in human ovarian endometrioid carcinomas (79). These previous observations suggested possible dual biological roles of the IGFBP3 signal pathways in various cancers (59-61,78,79). Nonetheless, our results showed a positive correlation between IGFBP3 protein expression and metastasis potential of the gastric cancer cells. Contrary to that reported in colorectal cancer HCT116 cells (80), we found in gastric cancer MKN45 cells that LGR4 expression was inversely correlated with the cell invasion ability.

A number of the genes identified in our studies have been verified for their transcriptional or translational activities in the mRNA or protein levels by semi-quantified RT-PCR and western blotting, respectively, such as TFF3, IGFBP3, BEX2, OTR, SGCE, LGR4, FANCA, MIA, and MPS1/TTK. FANCA has been reported to participate in the BRCA signaling pathway and is involved in the chromosome stability of cancer cells (81). MIA proteins binding to integrins promote detachment of melanoma cells from extracellular matrix structures and increase the migration ability of the cells, which could be inhibited by treatments with chemicals (82). MIA may play an important role in gastric tumor cell invasion and metastasis. The mRNA or protein expression profiles verified in the present study are in agreement with those previously observed.

In addition, we have also identified a number of novel genes, listed in Table V, using the same evaluation processes. These novel genes have not been previously demonstrated with any biological activity nor are they known with any cancer progression-related or tumor metastasis-associated activities. Similarly, these novel genes are likely to be involved in important biological processes in the development and progression of human gastric tumor invasion and metastasis. Their possible cellular/subcellular mechanisms involving tumor progression or metastasis are to be further explored in the future. By using gene-silencing approaches such as siRNA treatments to the MKN45-GFP-12 cells, one may further investigate the functional roles of the pro-metastasis genes in the tumor metastatic process and their underlying molecular mechanisms. For the genes against metastasis, one can restore the downregulated gene functions by gene transfection in MKN45-GFP-12 cells to demonstrate a decrease in their metastatic abilities. Furthermore, one can look into the gene expression levels in the clinical patient specimens and search for clinical relevance in terms of tumor progression as well as patient survival.

Furthermore, we established a highly aggressive MKN45-GFP-12 cell line and adopted an orthotopic model in which human gastric cancer cells of diffuse type were intraperitoneally inoculated in nude mice to mimic the pathological condition of peritoneal metastasis in patients. The malignancies of MKN45-GFP and MKN45-GFP-12 cells were compared using the orthotopic model. Compared

to MKN45-GFP cells, MKN45-GFP-12 cells tend to invade internal organs, such as the liver, and to cause ascites at a shorter onset time, indicating a higher malignant property of the MKN45-GFP-12 cells. More tumor nodules were growing in the abdominal cavity of MKN45-GFP-12-inoculated nude mice at Day 14 (data not show). By using an *in vivo* selection process, we previously established a human gastric cancer cell line MKN45-GFP-ip4 (38). Whether the two malignant cell lines MKN45-GFP12 and MKN45-GFP-ip4 established via the *in vitro* and *in vivo* selections, respectively, share a similar gene expression profile requires further investigation.

In this study, we established several human diffuse type gastric cancer cell sublines with different invasion abilities and identified a number of putative gastric tumor metastasis-associated genes, including novel genes without any known biological activity (GEO accession number GSE33570). These genes and protein products are to be further investigated for their roles in the molecular and cellular actions related to tumor metastasis. The molecular profiles of these identified genes, gene transcripts, and/or proteins in the patient specimens are likely to be useful for diagnostic, therapeutic, and/or prognostic purposes. In particular, they may be used as molecular targets for the development of drugs against tumor metastasis. These further research efforts could ultimately lead to the identification of tumor metastasis-associated molecules from which diagnostics and therapeutics for the human gastric cancer may be discovered.

Acknowledgements

This study was supported by the following grants, NHRI-BP-091-CF03, NHRI-BP-093-CB06, NHRI-BP-094-PP11, NHRI-BP-094-PP13, NHRI-095-PP07, and NSC-92-2218-E-400-001, awarded to C.T. Chen from The National Health Research Institutes, Miaoli and The National Science Council, Taiwan, R.O.C.

References

1. Archie V, Kauh J, Jones DV Jr, Cruz V, Karpeh MS Jr and Thomas CR Jr: Gastric cancer: standards for the 21st century. Crit Rev Oncol Hematol 57: 123-131, 2006.
2. Brenner H, Rothenbacher D and Arndt V: Epidemiology of stomach cancer. Methods Mol Biol 472: 467-477, 2009.
3. Yeh KH and Cheng AL: Recent advances in therapy for gastric cancer. J Formos Med Assoc 103: 171-185, 2004.
4. Parkin DM: The global health burden of infection-associated cancers in the year 2002. Int J Cancer 118: 3030-3044, 2006.
5. Vital and Health Statistics Division, Statistics and Information Department, Ministry of Health, Labour and Welfare: Vital statistics in Japan (1950-2007).
6. Horner MJ, Ries LAG, Krapcho M, Neyman N, Aminou R, Howlader N, Altekruse SF, Feuer EJ, Huang L, Mariotto A, Miller BA, Lewis DR, Eisner MP, Stinchcomb DG and Edwards BK (eds): SEER Cancer statistics review, 1975-2006. National Cancer Institute, Bethesda, 2008.
7. Lee KH, Lee JH, Cho JK, Kim TW, Kang YK, Lee JS, Kim WK, Chung JG, Lee IC and Sun HS: A prospective correlation of Laurén's histological classification of stomach cancer with clinicopathological findings including DNA flow cytometry. Pathol Res Pract 197: 223-229, 2001.
8. Whiting J, Sano T, Saka M, Fukagawa T, Katai H and Sasako M: Follow-up of gastric cancer: a review. Gastric Cancer 9: 74-81, 2006.
9. The EUROCARE-4 database on cancer survival in Europe [http://www.eurocare.it/Results/tabid/79/Default.aspx#eu4dB].
10. Guarino M: Epithelial-mesenchymal transition and tumour invasion. Int J Biochem Cell Biol 39: 2153-2160, 2007.
11. Wu CY, Wu MS, Chiang EP, Wu CC, Chen YJ, Chen CJ, Chi NH, Chen GH and Lin JT: Elevated plasma osteopontin associated with gastric cancer development, invasion and survival. Gut 56: 782-789, 2007.
12. Kuniyasu H, Yasui W, Yokozaki H, Kitadai Y and Tahara E: Aberrant expression of c-met mRNA in human gastric carcinomas. Int J Cancer 55: 72-75, 1993.
13. Ran Y, Peng L, Hu H, Yu L, Liu Q, Zhou Z, Sun YM, Sun LC, Pan J, Sun LX, Zhao P and Yang ZH: Secreted LOXL2 is a novel therapeutic target that promotes gastric cancer metastasis via the Src/FAK pathway. Carcinogenesis 30: 1660-1669, 2009.
14. Kim JH, Kim MA, Lee HS and Kim WH: Comparative analysis of protein expressions in primary and metastatic gastric carcinomas. Hum Pathol 40: 314-322, 2009.
15. Gravalos C and Jimeno A: HER2 in gastric cancer: a new prognostic factor and a novel therapeutic target. Ann Oncol 19: 1523-1529, 2008.
16. Sakashita K, Mimori K, Tanaka F, Kamohara Y, Inoue H, Sawada T, Hirakawa K and Mori M: Prognostic relevance of Tensin4 expression in human gastric cancer. Ann Surg Oncol 15: 2606-2613, 2008.
17. Yu G, Wang J, Chen Y, Wang X, Pan J, Li G, Jia Z, Li Q, Yao JC and Xie K: Overexpression of phosphorylated mammalian target of rapamycin predicts lymph node metastasis and prognosis of Chinese patients with gastric cancer. Clin Cancer Res 15: 1821-1829, 2009.
18. Nakayama H, Yasui W, Yokozaki H and Tahara E: Reduced expression of nm23 is associated with metastasis of human gastric carcinomas. Jpn J Cancer Res 84: 184-190, 1993.
19. Okada K, Shimura T, Suehiro T, Mochiki E and Kuwano H: Reduced galectin-3 expression is an indicator of unfavorable prognosis in gastric cancer. Anticancer Res 26: 1369-1376, 2006.
20. Li X, Zhang Y, Cao S, Chen X, Lu Y, Jin H, Sun S, Chen B, Liu J, Ding J, Wu K and Fan D: Reduction of TIP30 correlates with poor prognosis of gastric cancer patients and its restoration drastically inhibits tumor growth and metastasis. Int J Cancer 124: 713-721, 2009.
21. Hsu PI, Hsieh HL, Lee J, Lin LF, Chen HC, Lu PJ and Hsiao M: Loss of RUNX3 expression correlates with differentiation, nodal metastasis, and poor prognosis of gastric cancer. Ann Surg Oncol 16: 1686-1694, 2009.
22. Kim DY, Joo JK, Park YK, Ryu SY, Kim HS, Noh BK, Lee HK and Lee HJ: E-cadherin expression in early gastric carcinoma and correlation with lymph node metastasis. J Surg Oncol 96: 429-435, 2007.
23. Hippo Y, Yashiro M, Ishii M, Taniguchi H, Tsutsumi S, Hirakawa K, Kodama T and Aburatani H: Differential gene expression profiles of scirrhous gastric cancer cells with high metastatic potential to peritoneum or lymph nodes. Cancer Res 61: 889-895, 2001.
24. Wang J and Chen S: Screening and identification of gastric adenocarcinoma metastasis-related genes using cDNA microarray coupled to FDD-PCR. J Cancer Res Clin Oncol 128: 547-553, 2002.
25. Kim JM, Sohn HY, Yoon SY, Oh JH, Yang JO, Kim JH, Song KS, Rho SM, Yoo HS, Kim YS, Kim JG and Kim NS: Identification of gastric cancer-related genes using a cDNA microarray containing novel expressed sequence tags expressed in gastric cancer cells. Clin Cancer Res 11: 473-482, 2005.
26. Myllykangas S, Junnila S, Kokkola A, Autio R, Scheinin I, Kiviluoto T, Karjalainen-Lindsberg ML, Hollmén J, Knuutila S, Puolakkainen P and Monni O: Integrated gene copy number and expression microarray analysis of gastric cancer highlights potential target genes. Int J Cancer 123: 817-825, 2008.
27. Hippo Y, Taniguchi H, Tsutsumi S, Machida N, Chong JM, Fukayama M, Kodama T and Aburatani H: Global gene expression analysis of gastric cancer by oligonucleotide microarrays. Cancer Res 62: 233-240, 2002.
28. Inoue H, Matsuyama A, Mimori K, Ueo H, and Mori M: Prognostic score of gastric cancer determined by cDNA microarray. Clin Cancer Res 8: 3475-3479, 2002.
29. Hasegawa S, Furukawa Y, Li M, Satoh S, Kato T, Watanabe T, Katagiri T, Tsunoda T, Yamaoka Y and Nakamura Y: Genome-wide analysis of gene expression in intestinal-type gastric cancers using a complementary DNA microarray representing 23,040 genes. Cancer Res 62: 7012-7017, 2002.
30. Yang S, Jeung HC, Jeong HJ, Choi YH, Kim JE, Jung JJ, Rha SY, Yang WI and Chung HC: Identification of genes with correlated patterns of variations in DNA copy number and gene expression level in gastric cancer. Genomics 89: 451-459, 2007.

31. Chang W, Ma L, Lin L, Gu L, Liu X, Cai H, Yu Y, Tan X, Zhai Y, Xu X, *et al:* Identification of novel hub genes associated with liver metastasis of gastric cancer. Int J Cancer 125: 2844-2853, 2009.
32. Oue N, Aung PP, Mitani Y, Kuniyasu H, Nakayama H and Yasui W: Genes involved in invasion and metastasis of gastric cancer identified by array-based hybridization and serial analysis of gene expression. Oncology 69: 17-22, 2005.
33. Motoyama T, Hojo H and Watanabe H: Comparison of seven cell lines derived from human gastric carcinomas. Acta Pathol Jpn 36: 65-83, 1986.
34. Yokozaki H: Molecular characteristics of eight gastric cancer cell lines established in Japan. Pathol Int 50: 767-777, 2000.
35. Chu YW, Yang PC, Yang SC, Shyu YC, Hendrix MJ, Wu R and Wu CW: Selection of invasive and metastatic subpopulations from a human lung adenocarcinoma cell line. Am J Respir Cell Mol Biol 17: 353-360, 1997.
36. Huang YC, Chen CT, Chen SC, Lai PH, Liang HC, Chang Y, Yu LC and Sung HW: A natural compound (Ginsenoside Re) isolated from Panax Ginseng as a novel angiogenic agent for tissue regeneration. Pharm Res 22: 636-646, 2005.
37. Li WT, Hwang DR, Chen CP, Shen CW, Huang CL, Chen TW, Lin CH, Chang YL, Chang YY, Lo YK, *et al*: Synthesis and biological evaluation of N-heterocyclic indolyl glyoxylamides as orally active anticancer agents. J Med Chem 46: 1706-1715, 2003.
38. Tuan TF, Tsai ML, Yeh KC, Huang HC, Chung CT, Huang CL, Han CH, Chen CP, Wang MH, Shen CC, *et al*: Intravenous paclitaxel against metastasis of human gastric tumors of diffuse type. Cancer Chemother Pharmacol 66: 773-783, 2010.
39. Geiger TR and Peeper DS: Metastasis mechanisms. Biochim Biophys Acta 1796: 293-308, 2009.
40. Chen X, Leung SY, Yuen ST, Chu KM, Ji J, Li R, Chan AS, Law S, Troyanskaya OG, Wong J, So S, Botstein D and Brown PO: Variation in gene expression patterns in human gastric cancers. Mol Biol Cell 14: 3208-3215, 2003.
41. Hansson LE, Engstrand L, Nyrén O, Evans DJ Jr, Lindgren A, Bergström R, Andersson B, Athlin L, Bendtsen O and Tracz P: Helicobacter pylori infection: independent risk indicator of gastric adenocarcinoma. Gastroenterology 105: 1098-1103, 1993.
42. Piazuelo MB, Epplein M and Correa P: Gastric cancer: an infectious disease. Infect Dis Clin North Am 24: 853-869, 2010.
43. Ferreira AC, Isomoto H, Moriyama M, Fujioka T, Machado JC and Yamaoka Y: Helicobacter and gastric malignancies. Helicobacter 13 (Suppl 1): 28-34, 2008.
44. Suganuma M, Kuzuhara T, Yamaguchi K and Fujiki H: Carcinogenic role of tumor necrosis factor-alpha inducing protein of Helicobacter pylori in human stomach. J Biochem Mol Biol 39: 1-8, 2006.
45. Smith MG, Hold GL, Tahara E and El-Omar EM: Cellular and molecular aspects of gastric cancer. World J Gastroenterol 12: 2979-2990, 2006.
46. Chan AO, Lam SK, Wong BC, Wong WM, Yuen MF, Yeung YH, Hui WM, Rashid A and Kwong YL: Promoter methylation of E-cadherin gene in gastric mucosa associated with Helicobacter pylori infection and in gastric cancer. Gut 52: 502-506, 2003.
47. Iwamoto J, Mizokami Y, Takahashi K, Nakajima K, Ohtsubo T, Miura S, Narasaka T, Takeyama H, Omata T, Shimokobe K, Ito M, Takehara H and Matsuoka T: Expressions of urokinase-type plasminogen activator, its receptor and plasminogen activator inhibitor-1 in gastric cancer cells and effects of Helicobacter pylori. Scand J Gastroenterol 40: 783-793, 2005.
48. Schmausser B, Endrich S, Brändlein S, Schär J, Beier D, Müller-Hermelink HK and Eck M: The chemokine receptor CCR7 is expressed on epithelium of non-inflamed gastric mucosa, Helicobacter pylori gastritis, gastric carcinoma and its precursor lesions and up-regulated by H. pylori. Clin Exp Immunol 139: 323-327, 2005.
49. Yasumoto K, Koizumi K, Kawashima A, Saitoh Y, Arita Y, Shinohara K, Minami T, Nakayama T, Sakurai H, Takahashi Y, Yoshie O and Saiki I: Role of the CXCL12/CXCR4 axis in peritoneal carcinomatosis of gastric cancer. Cancer Res 66: 2181-2187, 2006.
50. Zhao C, Lu X, Bu X, Zhang N and Wang W: Involvement of tumor necrosis factor-alpha in the upregulation of CXCR4 expression in gastric cancer induced by Helicobacter pylori. BMC Cancer 10: 419, 2010.
51. Amoh Y, Katsuoka K and Hoffman RM: Color-coded fluorescent protein imaging of angiogenesis: the AngioMouse models. Curr Pharm Des 14: 3810-3819, 2008.
52. Bouvet M, Tsuji K, Yang M, Jiang P, Moossa AR and Hoffman RM: In vivo color-coded imaging of the interaction of colon cancer cells and splenocytes in the formation of liver metastases. Cancer Res 66: 11293-11297, 2006.
53. Hoffman RM: The multiple uses of fluorescent proteins to visualize cancer in vivo. Nat Rev Cancer 5: 796-806, 2005.
54. Hoffman RM: Dual-color imaging of tumor angiogenesis. Methods Mol Biol 515: 45-61, 2009.
55. Chen JJ, Peck K, Hong TM, Yang SC, Sher YP, Shih JY, Wu R, Cheng JL, Roffler SR, Wu CW and Yang PC: Global analysis of gene expression in invasion by a lung cancer model. Cancer Res 61: 5223-5230, 2001.
56. Chen HY, Yu SL, Chen CH, Chang GC, Chen CY, Yuan A, Cheng CL, Wang CH, Terng HJ, Kao SF, *et al*: A five-gene signature and clinical outcome in non-small-cell lung cancer. N Engl J Med 356: 11-20, 2007.
57. Dhar DK, Wang TC, Tabara H, Tonomoto Y, Maruyama R, Tachibana M, Kubota H and Nagasue N: Expression of trefoil factor family members correlates with patient prognosis and neoangiogenesis. Clin Cancer Res 11: 6472-6478, 2005.
58. Rodrigues S, Van Aken E, Van Bocxlaer S, Attoub S, Nguyen QD, Bruyneel E, Westley BR, May FE, Thim L, Mareel M, Gespach C and Emami S: Trefoil peptides as proangiogenic factors in vivo and in vitro: implication of cyclooxygenase-2 and EGF receptor signaling. FASEB J 17: 7-16, 2003.
59. Liu B, Lee KW, Anzo M, Zhang B, Zi X, Tao Y, Shiry L, Pollak M, Lin S and Cohen P: Insulin-like growth factor-binding protein-3 inhibition of prostate cancer growth involves suppression of angiogenesis. Oncogene 26: 1811-1819, 2007.
60. Akhtar S, Meeran SM, Katiyar N and Katiyar SK: Grape seed proanthocyanidins inhibit the growth of human non-small cell lung cancer xenografts by targeting insulin-like growth factor binding protein-3, tumor cell proliferation, and angiogenic factors. Clin Cancer Res 15: 821-831, 2009.
61. Hansel DE, Rahman A, House M, Ashfaq R, Berg K, Yeo CJ and Maitra A: Met proto-oncogene and insulin-like growth factor binding protein 3 overexpression correlates with metastatic ability in well-differentiated pancreatic endocrine neoplasms. Clin Cancer Res 10: 6152-6158, 2004.
62. Saaristo A, Karpanen T and Alitalo K: Mechanisms of angiogenesis and their use in the inhibition of tumor growth and metastasis. Oncogene 19: 6122-6129, 2000.
63. Iwai K, Hirata K, Ishida T, Takeuchi S, Hirase T, Rikitake Y, Kojima Y, Inoue N, Kawashima S and Yokoyama M: An anti-proliferative gene BTG1 regulates angiogenesis in vitro. Biochem Biophys Res Commun 316: 628-635, 2004.
64. Fisk HA, Mattison CP and Winey M: A field guide to the Mps1 family of protein kinases. Cell Cycle 3: 439-442, 2004.
65. Dorer RK, Zhong S, Tallarico JA, Wong WH, Mitchison TJ and Murray AW: A small-molecule inhibitor of Mps1 blocks the spindle-checkpoint response to a lack of tension on mitotic chromosomes. Curr Biol 15: 1070-1076, 2005.
66. Poss KD, Nechiporuk A, Stringer KF, Lee C and Keating MT: Germ cell aneuploidy in zebrafish with mutations in the mitotic checkpoint gene mps1. Genes Dev 18: 1527-1532, 2004.
67. Takayama T, Miyanishi K, Hayashi T, Sato Y and Niitsu Y: Colorectal cancer: genetics of development and metastasis. J Gastroenterol 41: 185-192, 2006.
68. Naderi A, Liu J and Bennett IC: BEX2 regulates mitochondrial apoptosis and G1 cell cycle in breast cancer. Int J Cancer 126: 1596-1610, 2010.
69. Chen PS, Wang MY, Wu SN, Su JL, Hong CC, Chuang SE, Chen MW, Hua KT, Wu YL, Cha ST, *et al:* CTGF enhances the motility of breast cancer cells via an integrin-alphavbeta3-ERK1/2-dependent S100A4-upregulated pathway. J Cell Sci 120: 2053-2065, 2007.
70. Bracke ME, Van Roy FM and Mareel MM: The E-cadherin/catenin complex in invasion and metastasis. Curr Top Microbiol Immunol 213: 123-161, 1996.
71. Mauro L, Bartucci M, Morelli C, Ando S and Surmacz E: IGF-I receptor-induced cell-cell adhesion of MCF-7 breast cancer cells requires the expression of junction protein ZO-1. J Biol Chem 276: 39892-39897, 2001.
72. Qin J, Feng M, Wang C, Ye Y, Wang PS and Liu C: Oxytocin receptor expressed on the smooth muscle mediates the excitatory effect of oxytocin on gastric motility in rats. Neurogastroenterol Motil 21: 430-438, 2009.
73. Morita T, Shibata K, Kikkawa F, Kajiyama H, Ino K and Mizutani S: Oxytocin inhibits the progression of human ovarian carcinoma cells in vitro and in vivo. Int J Cancer 109: 525-532, 2004.

74. Meyer zum Büschenfelde D, Hoschützky H, Tauber R and Huber O: Molecular mechanisms involved in TFF3 peptide-mediated modulation of the E-cadherin/catenin cell adhesion complex. Peptides 25: 873-883, 2004.
75. Ortega P, Moran A, Fernandez-Marcelo T, De Juan C, Frias C, Lopez-Asenjo JA, Sanchez-Pernaute A, Torres A, Diaz-Rubio E, Iniesta P and Benito M: MMP-7 and SGCE as distinctive molecular factors in sporadic colorectal cancers from the mutator phenotype pathway. Int J Oncol 36: 1209-1215, 2010.
76. Patarroyo M, Tryggvason K and Virtanen I: Laminin isoforms in tumor invasion, angiogenesis and metastasis. Semi Cancer Biol 12: 197-207, 2002.
77. Wang J, Levenson AS and Satcher RL Jr: Identification of a unique set of genes altered during cell-cell contact in an *in vitro* model of prostate cancer bone metastasis. Int J Mol Med 17: 849-856, 2006.
78. Xi Y, Nakajima G, Hamil T, Fodstad O, Riker A and Ju J: Association of insulin-like growth factor binding protein-3 expression with melanoma progression. Mol Cancer Ther 5: 3078-3084, 2006.
79. Torng PL, Lee YC, Huang CY, Ye JH, Lin YS, Chu YW, Huang SC, Cohen P, Wu CW and Lin CT: Insulin-like growth factor binding protein-3 (IGFBP-3) acts as an invasion-metastasis suppressor in ovarian endometrioid carcinoma. Oncogene 27: 2137-2147, 2007.
80. Gao Y, Kitagawa K, Hiramatsu Y, Kikuchi H, Isobe T, Shimada M, Uchida C, Hattori T, Oda T, Nakayama K, Nakayama KI, Tanaka T, Konno H and Kitagawa M: Up-regulation of GPR48 induced by down-regulation of p27Kip1 enhances carcinoma cell invasiveness and metastasis. Cancer Res 66: 11623-11631, 2006.
81. D'Andrea AD and Grompe M: The Fanconi anaemia/BRCA pathway. Nat Rev Cancer 3: 23-34, 2003.
82. Schmidt J and Bosserhoff AK: Processing of MIA protein during melanoma cell migration. Int J Cancer 125: 1587-1594, 2009.